Journal of Applied Polymer Science

Flame-Retardant Materials Based on Phosphorus-Containing Polyhedral Oligomeric Silsesquioxane and Bismaleimide/Diallylbisphenol A with Improved Thermal Resistance and Dielectric Properties

Zheng Wang, Wei Wu, Yuhua Zhong, Mingzhu Ruan, Lin Lin Hui
Sino-German Joint Research Center of Advanced Materials, School of Materials Science and Engineering, East China University of Science and Technology, Shanghai 200237, China
Correspondence to: W. Wu (E-mail: wuwei@ecust.edu.cn)

ABSTRACT: Polyhedral oligomeric silsesquioxane containing 9,10-dihydro-9-oxa-10-phosphaphenanthrene-10-oxide (DP) was used to flame-retard 4,4′-bismaleimidophenyl methane (BDM)/2,2′-dially bisphenol A (DBA) resins, and the integrated properties of the resins were investigated. The fire resistance of BDM/DBA resins containing DP was analyzed by limiting oxygen index (LOI) and vertical burning (UL94) tests. The results show that DP increased the LOI of the resins from 25.3 to 38.5%. The BDM/DBA resins were evaluated to have a UL-94 V-1 rating, which did not satisfy the high standards of industry. On the other hand, BDM/DBA containing DP achieved a UL-94 V-0 rating. The thermal stability and char formation were studied by thermogravimetric analysis (TGA) and Fourier transform infrared spectroscopy. TGA and scanning electron microscopy–energy-dispersive X-ray spectrometry measurements demonstrated that the DP resulted in an increase in the char yield and the formation of the thermally stable carbonaceous char. The results of Raman spectroscopy showed that the DP enhanced the graphitization degree of the resin during combustion. Moreover, the modified BDM/DBA resins exhibited improved dielectric properties. Specifically, the dielectric constant and loss at 1 MHz of the BDM/DBA/15% DP resin were 3.11 and 0.008, respectively, only about 93 and 73% of those of the BDM/DBA resin. All of the investigations showed that DP was an effective additive for developing high-performance resins with attractive flame-retardant and dielectric properties. © 2014 Wiley Periodicals, Inc. J. Appl. Polym. Sci. **2015**, *132*, 41545.

KEYWORDS: flame retardance; resins; thermosets

Received 1 July 2014; accepted 19 September 2014
DOI: 10.1002/app.41545

INTRODUCTION

Bismaleimide (BMI) resins are widely used as matrixes of high-performance composites in the fields of aerospace, transportation, machinery, and electronics. This kind of resin has excellent properties, including good thermal stability, good processability, high mechanical strength, excellent dielectric properties, and so on.[1–3] However, as for most organic resins, their poor flame retardancy is one of the drawbacks of BMI resins. To meet the strict requirements of cutting-edge fields, it is necessary to improve the flammability properties of these resins. Many efforts have been made to improve the flame retardancy of the resins, and lots of valuable results have been achieved so far.[4–6]

Generally, the use of halogen-containing fire retardants used to be considered an effective approach. However, there has been increasing interests in the use of halogen-free flame-retarding substances. Many more studies on phosphorus- and silicone-based retardants[7–12] have been reported. 9,10-Dihydro-9-oxa-10-phosphaphenanthrene-10-oxide (DOPO) is an important phosphorus flame retardant with a high thermal stability, good oxidation, and good oxidation resistance.[13,14] Furthermore, some researchers have reported that systems that contain both phosphorus- and silicone-based retardants display better flame-retardant properties because of the phosphorus–silicon synergism.[15,16]

Inorganic–organic hybrid polyhedral oligomeric silsesquioxanes (POSSs) have a chemical composition ($RSiO_{1.5}$) with different R groups, including hydrogen or any alkyl, alkylene, aryl, or arylene group, or organofunctional derivatives.[17,18] POSS molecules with nanosized, cage-shaped, three-dimensional structures can be incorporated into almost all kinds of thermosetting polymers or thermoplastics by grafting, blending, crosslinking, or copolymerization.[19,20] In recent years, the use of POSS as a flame retardant in resins has attracted more and more attention.[21,22]

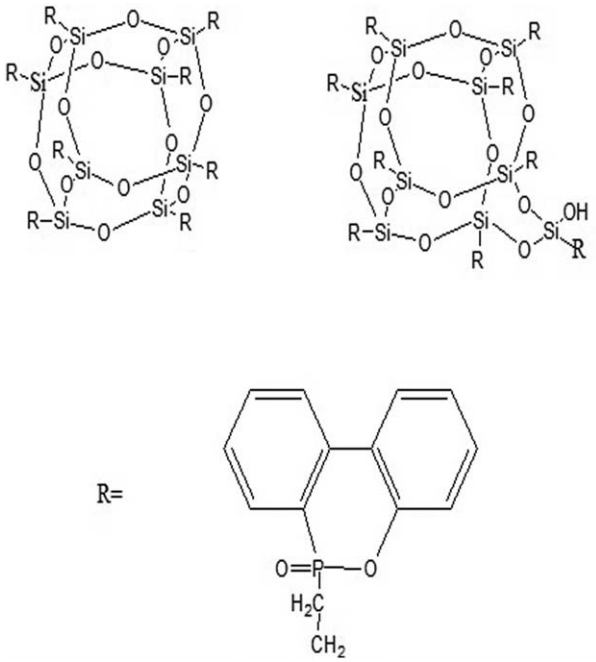

Scheme 1. Typical chemical structures of the DP molecules.

A DOPO-containing POSS (Scheme 1) was synthesized successfully.[23] This is a novel, phosphorus-containing POSS had an excellent thermal stability. Yang's group investigated the pyrolysis and fire behavior of epoxy/DP resins[24] and discovered an interesting blowing-out effect.[25] They concluded that it was a good halogen-free flame retardant for polymers[26,27] and demonstrated that the synergistic effect of the silicon and phosphorus flame-retardant epoxy resin showed a good performance. However, its effect on the flame retardancy of the 4,4′-bismaleimidophenyl methane (BDM)/2,2′-dially bisphenol A (DBA) resin was not reported. Also, the influence of this kind of flame retardant on the dielectric properties has seldom been discussed.

In this article, we report first on the preparation of a novel resin based on BDM/DBA resin and DP and the thermal degradation behaviors of the BDM/DBA/DP resins. The flame retardancy, thermal stability, and dielectric properties of the BDM/DBA/DP resins were studied. The aim of the research reported in this article was to find a new approach for developing high-performance flame-retardant resins with improved thermal resistance and dielectric properties.

EXPERIMENTAL

Materials

BDM was obtained from Hubei ShuangFei Chemical Co., Ltd. (China). DBA was purchased from Laiyu Chemical Factory (China). Azobisisobutyronitrile (99.5%) and concentrated hydrochloric acid (HCl; 36.5%) were purchased from LingFeng Chemical Co., Ltd. DOPO was obtained from Eutec Trading (Shanghai) Co., Ltd. (China). Vinyltriethoxysilane (VTES) was purchased from Nanjing Up Chemical Co., Ltd. (China). Distilled water was produced in our laboratory.

Synthesis of DP

The DP was synthesized according to a previous study.[23] The addition reaction between VTES (10 g) and DOPO (10.8 g) was initiated by azobisisobutyronitrile and led to the DOPO-containing triethoxysilane (DOPO–VTES). The hydrolytic condensation of DOPO–VTES (19.7 g) was performed in a methanol solution with HCl as a catalyst. The temperature was held at 80°C for 24 h. The crude product was obtained as a white powder after suction filtration and rinsing with deionized water (8.6 g, 44% yield)

Preparation of the Prepolymers and Cured Resins

According to Table I, appropriate amounts of DBA and DP, DOPO were thoroughly blended at 125–135°C until a clear yellow liquid was obtained. Then, preweighed BDM was added to the beaker at 125–135°C with stirring until a transparent liquid was formed; this liquid was kept at that temperature for 15 min to obtain a homogeneous liquid, coded as BDM/DBA/*n*DP, where *n* means is weight loading of DP in the prepolymer and DP means DOPO-POSS.

Each prepolymer was thoroughly degassed at 135°C and poured into a preheated (135°C) metal mold; this was followed by curing and postcuring following the process of 150°C for 2 h, 180°C for 2 h, 200°C for 2 h, and 230°C for 4 h.

Measurements

^{1}H-NMR measurement was performed on Bruker Avance 400 spectrometer at room temperature with $CDCl_3$ as a solvent.

Fourier transform infrared (FTIR) spectra were recorded between 400 and 4000 cm^{-1} at a resolution of 2 cm^{-1} on a Nicolet-6700 infrared spectrometer.

Scanning electron microscopy (SEM; S-4800, Japan) coupled with energy-dispersive X-ray spectrometry (EDS) was used to observed the morphologies of the fractured surfaces of the charred sample layers.

Thermogravimetric analysis (TGA) was performed with a PerkinElmer Pyris instrument in the range from 25 to 800°C at a heating rate of 20°C/min.

UL94 tests were performed according to ASTM D 63–77. The dimensions of each sample were $(125 \pm 0.02) \times (13 \pm 0.02) \times (3 \pm 0.02)$ mm^3. The reported results are the average of five measurements.

The limiting oxygen index (LOI) values were measured on a Stanton Redcraft flame meter (United Kingdom) according to

Table I. Formulations of the BDM/DBA, BDM/DBA/*n*DP, and BDM/DBA/DOPO Resins

Resin	BDM/DBA (wt %)	DP (wt %)
BDM/DBA	100	—
BDM/DBA/5% DP	95	5
BDM/DBA/10% DP	90	10
BDM/DBA/15% DP	85	15
BDM/DBA/10% DOPO	90	10

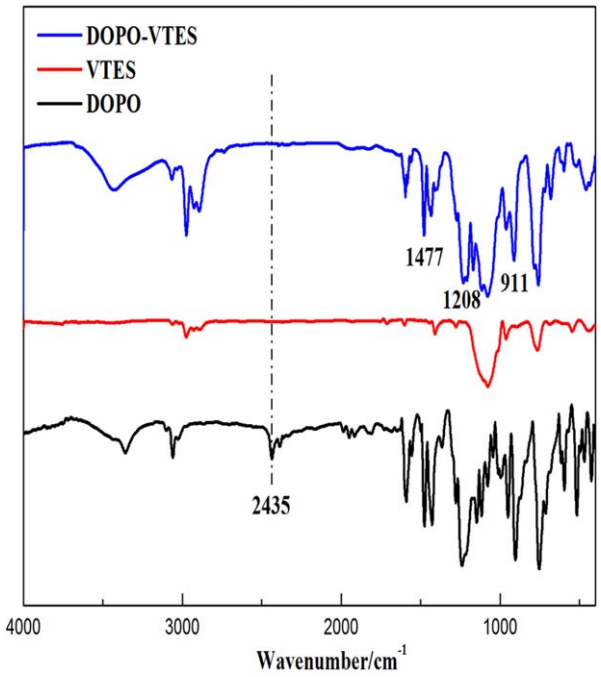

Figure 1. FTIR spectra of DOPO, VTES, and DOPO–VTES. [Color figure can be viewed in the online issue, which is available at wileyonlinelibrary.com.]

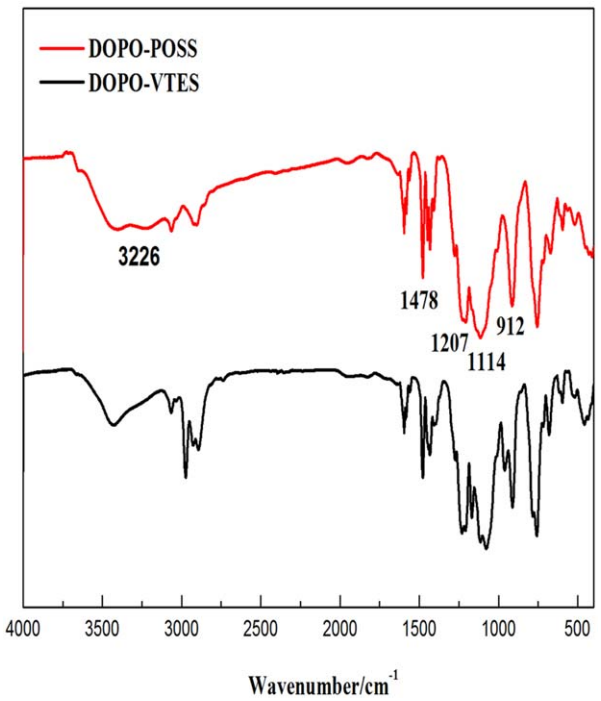

Figure 3. FTIR spectra of DOPO–VTES and DP. [Color figure can be viewed in the online issue, which is available at wileyonlinelibrary.com.]

ASTM D 2863/77. The dimensions of each sample were $(100 \pm 0.02) \times (6.5 \pm 0.02) \times (3 \pm 0.02)$ mm^3. The reported results are the average of three measurements.

Raman spectroscopy measurements were carried out at room temperature with a Thermo Fisher Scientific DXR laser Raman spectrometer with excitation provided in backscattering geometry by a 780-nm argon laser line.

The dielectric properties of each sample was tested with a Novocontrol Concept 40 apparatus (Germany) between 1 Hz and 1 MHz at room temperature.

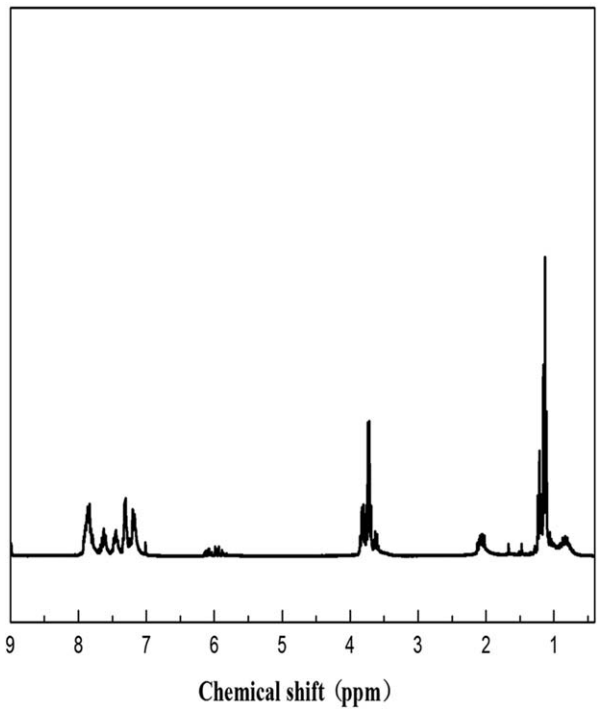

Figure 2. ^{1}H-NMR spectra of DOPO–VTES.

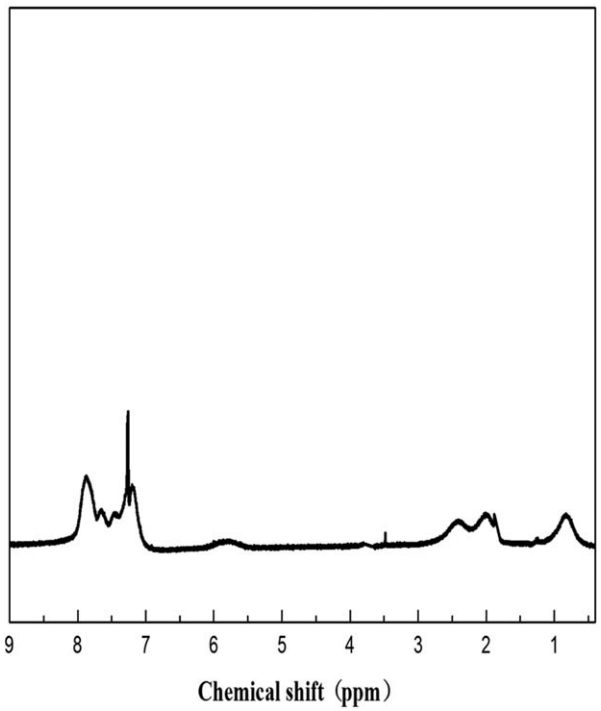

Figure 4. ^{1}H-NMR spectra of DP.

Table II. Results of the LOI and UL-94 Tests of the Investigated Formulations

Sample	LOI (%)	Ranking	Dripping[a]	t_1/t_2 (s)
BDM/DBA	25.3 ± 0.5	V-1	No/no	5.0/13.4
BDM/DBA/5% DP	34.5 ± 0.5	V-1	No/no	3.0/13.1
BDM/DBA/10% DP	35.9 ± 0.5	V-0	No/no	2.6/5.3
BDM/DBA/15% DP	38.5 ± 0.5	V-0	No/no	2.2/2.5
BDM/DBA/10% DOPO	34.8 ± 0.5	V-1	No/no	4.8/12.3

[a] First flame application/second flame application.

RESULTS AND DISCUSSION

Characterization

The chemical structure of DOPO–VTES was characterized by FTIR spectroscopy and ^{1}H-NMR. The FTIR spectra of DOPO, VTES, and DOPO–VTES are shown in Figure 1. Compared with that of the pure DOPO, the absorbance peak at 2435 cm^{-1} for the P—H bond of DOPO disappeared completely; this indicated the complete reaction of DOPO. The peak at 911 cm^{-1} corresponded to the stretching vibration of P—O—Ph, and the peak at 1208 cm^{-1} belonged to the stretching vibration of P═O. Moreover, the peak at 1477 cm^{-1} indicated the existence of the P–phenyl bond. The ^{1}H-NMR spectrum of DOPO–VTES is shown in Figure 2. The peak at 8.68 ppm for the P—H bond of DOPO disappeared completely. In addition, the peaks at 0.86 and 2.1 ppm for the DOPO–VTES were ascribed to methylene protons in Si—CH_2 and P—CH_2, respectively.

The chemical structure of DP was characterized by FTIR spectroscopy and ^{1}H-NMR.

The FTIR spectra of DOPO–VTES and DP are shown in Figure 3. In the FTIR spectrum of DP, the absorbance peaks of —O—CH_2—CH_2—CH_3 at 963, 2888, 2925, and 2975 cm^{-1} almost disappeared. The strong absorbance band at 1114 cm^{-1} were ascribed to the formation of the Si—O—Si bonds, and the peak at 3226 cm^{-1} belonged to Si—OH. The ^{1}H-NMR of DP is shown in Figure 4. The peaks at 1.2–1.26 and 3.83–3.88 ppm, ascribed to methyl and methene protons in O—CH_2—CH_3, of DOPO–VTES disappeared in the spectrum of DP. The peak at 3.46 ppm was ascribed to Si—OH in DP.

Flame-Retardant Properties

The results of flammability (the LOI and the UL94 tests) are given in Table II for all of the investigated samples. In the UL 94 tests, the BDM/DBA resin burned easily. However, the LOI value of the BDM/DBA resin increased to 34.8%, and the UL 94 rating improved to V-1 with the addition of 10 wt % DOPO. The conclusion conformed with those in the reported literature. Li et al.[28] investigated the flame-retardancy effects of phosphorus-containing compounds on epoxy resins, and their LOI value increased with the addition of phosphorus-based retardants. The same weight of DOPO was replaced by DP in the BDM/DBA/10% DP resin. As a result, the LOI value increased to 35.9%. In

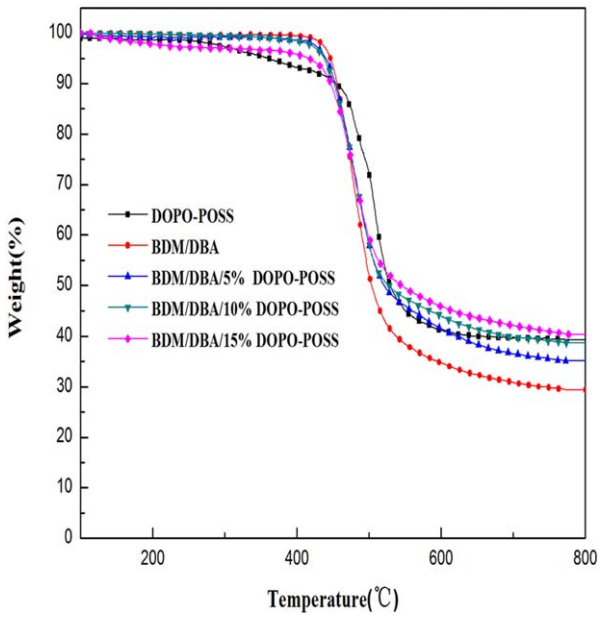

Figure 5. TGA curves of BDM/DBA resins with various contents of DP under a nitrogen atmosphere. [Color figure can be viewed in the online issue, which is available at wileyonlinelibrary.com.]

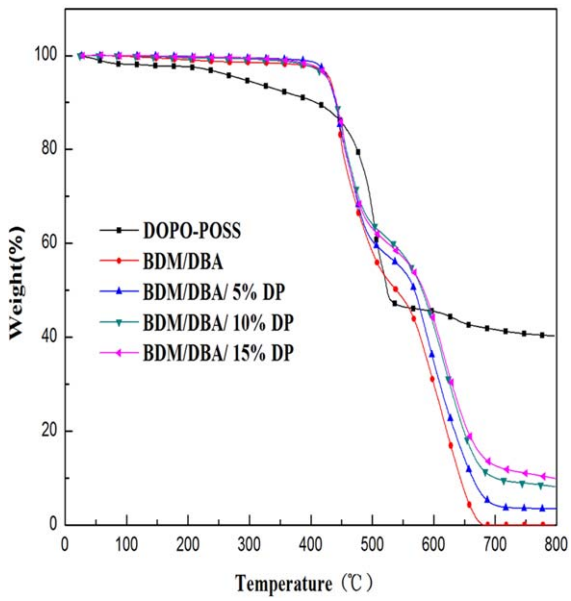

Figure 6. TGA curves of BDM/DBA resins with various contents of DP under an air atmosphere. [Color figure can be viewed in the online issue, which is available at wileyonlinelibrary.com.]

Table III. TGA Data for the Samples in Nitrogen

Sample	$T_{-5\%}$ (°C)	$T_{-50\%}$ (°C)	Char residue at 800°C in experiment (%)	Char residue at 800°C in theory (%)
DP	360.2	529.8	39.3	39.3
BDM/DBA	446.2	503.4	29.4	29.4
BDM/DBA/5% DP	439.3	520.9	35.1	29.9
BDM/DBA/10% DP	437.8	526.8	38.7	30.4
BDM/DBA/15% DP	416.5	544.4	40.4	30.9

addition, the combination of DOPO and POSS resulted in a V-0 ranking. The results suggest that a synergistic effect probably existed between DOPO and POSS.

We observed that the LOI values of BDM/DBA/DP increased obviously with the content of DP. When 15 wt % DP was added, the LOI value of the BDM/DBA/DP resin leveled up from 25.3 to 38.5%. The flame-retarding level of the cured BDM/DBA resins was V-1; however, when the content of DP increased to 10 wt %, the flame retardancy of the cured BDM/DBA/DP resins was classified as UL-94 V-0. With increasing DP content, the average combustion times after the first and second applications of the flame (t_1 and t_2, respectively) in the UL-94 testing decreased gradually, and self-extinguishing was observed with samples loaded with 5, 10, and 15 wt % DP. The results from the tests show that DP flame-retarded the BDM/DBA resins effectively; this was probably due to the fact that the DP contained both phosphorous and silicon elements, as shown Scheme 1. The DOPO groups in DP acted similarly to aromatic phosphates, which impart flame retardancy through flame inhibition in the gas phase and char enhancement in the condensed phase.[29,30] In the gas phase, phosphorus-containing flame retardants promote pyrolysis of the PO radical and HPO, which can react with the H&fradic; and &fradic;OH radicals. In the condensed phase, they promote char formation, which acts as a barrier. On the other hand, silicon tends to form a silicon dioxide layer to protect the resin during burning.[31,32]

Thermal Stability

TGA is an effective method for characterizing the thermooxidation resistance of materials. Figures 5 and 6 provide the TGA curves of the BDM/DBA resins with various contents of DP under nitrogen and air atmospheres, respectively. The temperature of 5 wt % weight loss ($T_{-5\%}$), the midpoint temperature of degradation ($T_{-50\%}$), and the fraction of the solid residue (Y_c) at 800°C were obtained from the TGA curves. All of these data are presented in Tables III and IV.

As shown in Figure 5, the thermal degradation process of all the samples had one stage as the BDM/DBA. We found that the $T_{-5\%}$ of the BDM/DBA/DP resins was lower than that of the BDM/DBA resin with increasing DP load. The reason was probably that the initial degradation of the DP began at a low temperature. However, we noticed that the $T_{-50\%}$ of the BDM/DBA/DP resins was higher than that of BDM/DBA; this resulted from the fact that DP could form a ceramic-like layer under a nitrogen atmosphere and the layer could protect the inner part of the resins from further degradation. The char residues increased gradually when the content of DP rose from 5 to 15 wt %. The thermogravimetric data showed that the Y_c of BDM/DBA at 800°C was 29.4%, but that of BDM/DBA/15% DP was 40.4%. All of the values of the char residues in the experiment were higher the theoretical values. The high Y_c was attributed to the synergistic effect of phosphorous and silicon; this indicated that phosphorous accelerated the formation of char, whereas silicon kept the char from undergoing thermal degradation.[33]

Figure 6 shows the TGA curves of the DP, BDM/DBA, BDM/DBA/5% DP, BDM/DBA/10% DP, and BDM/DBA/15% DP in an air atmosphere. For the BDM/DBA/DP resins, the thermooxidative degradation process had two stages. The $T_{-5\%}$ values of the BDM/DBA/DP resins were almost the same as that of the BDM/DBA resin. As shown in Figure 6, the first mass loss regions for the BDM/DBA and BDM/DBA/DP resins were 400–512°C. DP did not show an obvious effect on the improvements of the thermal stability of the BDM/DBA/DP resins in this temperature region. The residues of the BDM/DBA and BDM/DBA/DP resins at 480°C showed similar values, about 66%. Then, the second degradation stage was at 544–709°C. The $T_{-50\%}$ values of the BDM/DBA/DP resins were higher than those of the BDM/DBA resins; that is, DP could be

Table IV. TGA Data for the Samples in Air

Sample	$T_{-5\%}$ (°C)	$T_{-50\%}$ (°C)	Char residue at 800°C in experiment (%)	Char residue at 800°C in theory (%)
DP	289.7	525.6	40.2	40.2
BDM/DBA	431.6	537.0	0	0
BDM/DBA/5% DP	429.8	569.3	3.4	2.0
BDM/DBA/10% DP	429.4	580.6	8.1	4.0
BDM/DBA/15% DP	429.5	585.1	9.9	6.0

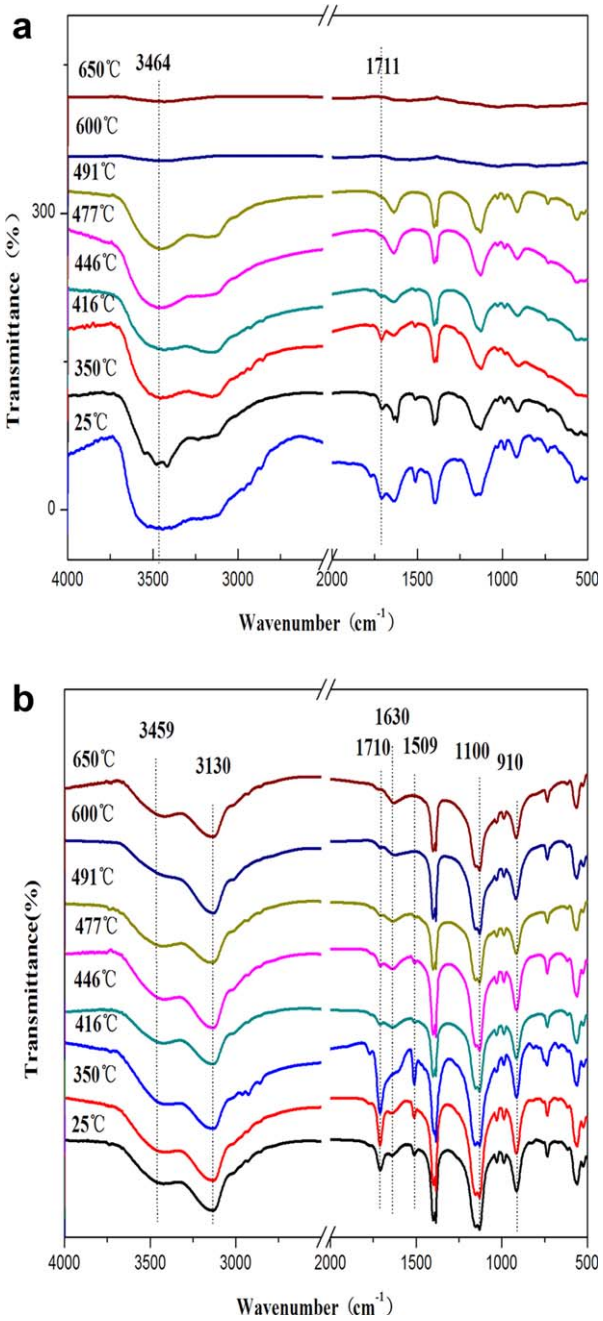

Figure 7. FTIR spectra of (a) BDM/DBA and (b) BDM/DBA/15% DP resins degraded at different temperatures for 15 min in an air atmosphere. [Color figure can be viewed in the online issue, which is available at wileyonlinelibrary.com.]

oxidized and form a silicon dioxide layer. The silicon dioxide layer could improve the thermooxidation resistance of the BDM/DBA resins. As the content of DP rose from 0 to 15%, the char residues increased gradually. The char yield of the BDM/DBA resin at 800°C was 0%. However, that of BDM/DBA/15% DP was 9.9%. We observed that DP played an important role in the char formation of the BDM/BDA/DP resins under an air atmosphere. Some researchers have reported that a thick charred layer is a good thermal barrier that can delay and prevent the thermooxidative degradation of the resin; therefore, a high Y_c will give the resin system excellent flame-retardant properties.

Thermooxidative Degradation

To study the effect of DP on the flame retardancy of the BDM/DBA resin, the change in chemical structure during the thermooxidative degradation of BDM/DBA and BDM/DBA/15% DP resins was monitored by FTIR, and the corresponding spectra are shown in Figure 7.

As for the BDM/DBA resin, we observed that the peaks around 3459, 3130, 1710, 1630, and 1509 cm^{-1} were the characteristic absorptions of BDM/DBA. The relative areas of the characteristic absorptions for the BDM/DBA resin decreased with the temperature and almost disappeared at about 600°C; this demonstrated that the organic resin was decomposed. However, all of those peaks could still be found after the temperature was maintained at 650°C for 15 min; this implied that the DP could protect the resin from complete decomposition.

In addition, in the characteristic absorptions of the organic bonds in the FTIR spectrum of the BDM/DBA/15% DP resin after it was maintained at 650°C, there were absorptions reflecting Si—O—Si (1100 cm^{-1}) and P—O—C (910 cm^{-1}). It is known that organic silicon resin-based materials can form a protective barrier during burning to ensure a matrix with superior thermal stability.[34]

Morphology of the Char Layer

Figure 8 shows a photograph of the BDM/DBA and BDM/DBA/15% DP resins after they were maintained at 800°C for 15 min in a muffle furnace. The shape of the BDM/DBA resin was obviously destroyed after the resin was maintained at 800°C for 15 min. Instead, as the temperature increased, the char of the

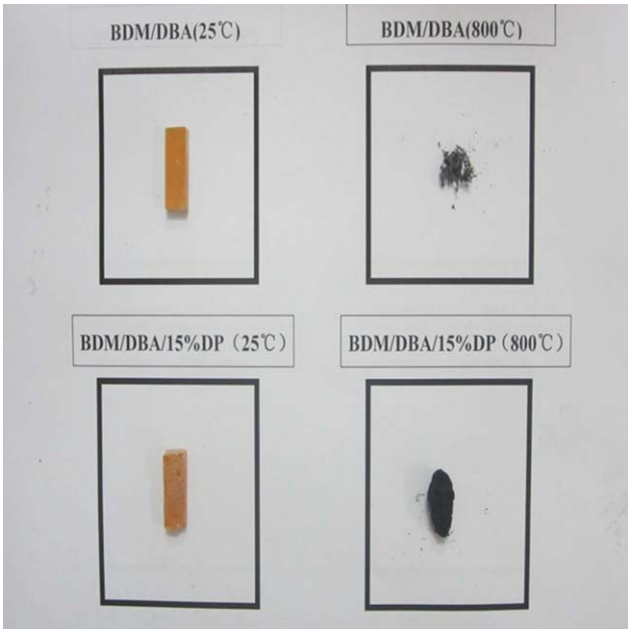

Figure 8. Photograph of the BDM/DBA and BDM/DBA/15% DP resins. [Color figure can be viewed in the online issue, which is available at wileyonlinelibrary.com.]

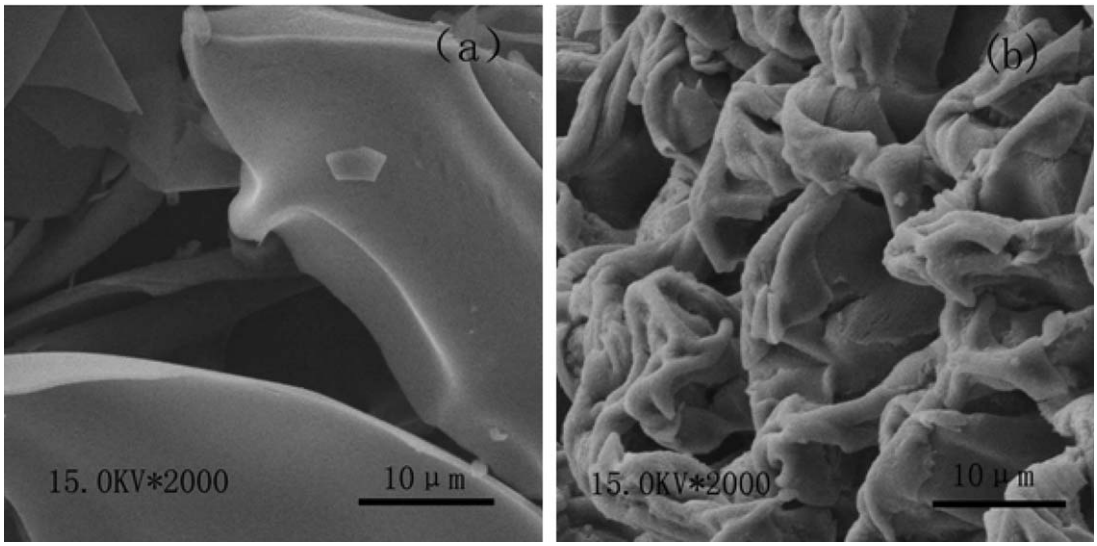

Figure 9. SEM micrographs of the residuals chars for (a) BDM/DBA and (b) BDM/DBA/15% DP resins.

Table V. Elemental Compositions of the Residues for the BDM/DBA and BDM/DBA/15% DP Resins

Sample	Elemental concentration (%)				
	C	O	N	Si	P
BDM/DBA	78.15	12.33	9.62	—	—
BDM/DBA/15% DP	53.59	34.01	6.48	3.83	2.08

BDM/DBA resin collapsed; this demonstrated that the carbon produced during the composition did not form a compact layer, and thus, the resin could not be well protected from decomposition. In contrast, the BDM/DBA/15% DP resin showed a different phenomenon. We observed that the char from the BDM/DBA/15% DP resin was firm and retained its shape after it was maintained at 800°C for 15 min. Moreover, the mass of the residue significantly increased. To further investigate the reason for this phenomenon, the microstructure of the carbon layers was investigated.

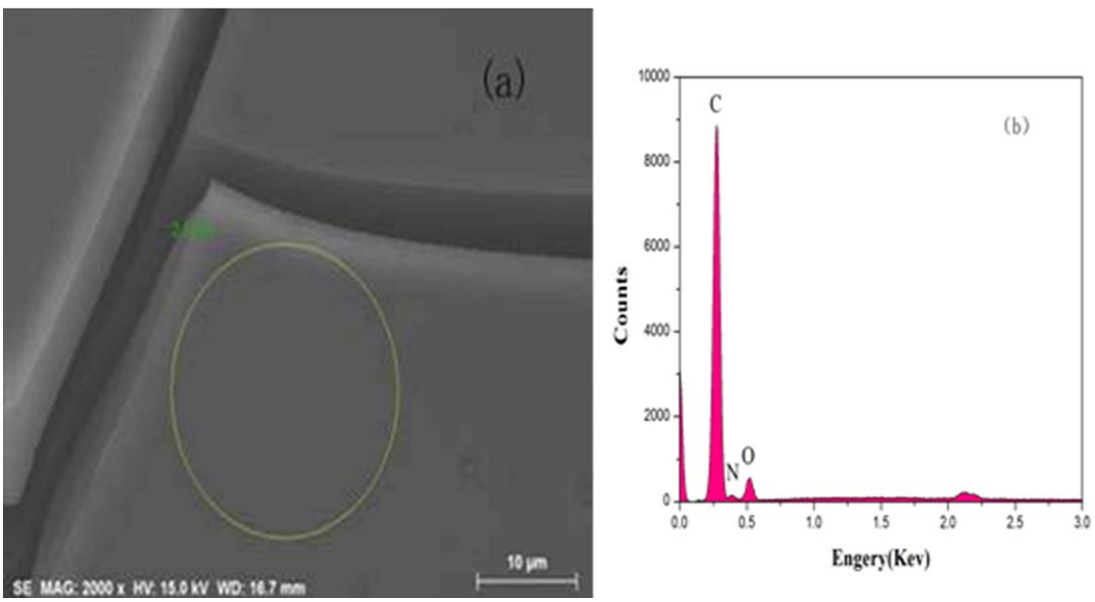

Figure 10. (a) SEM images and (b) EDS mapping pictures of the residue for the BDM/DBA resin. [Color figure can be viewed in the online issue, which is available at wileyonlinelibrary.com.]

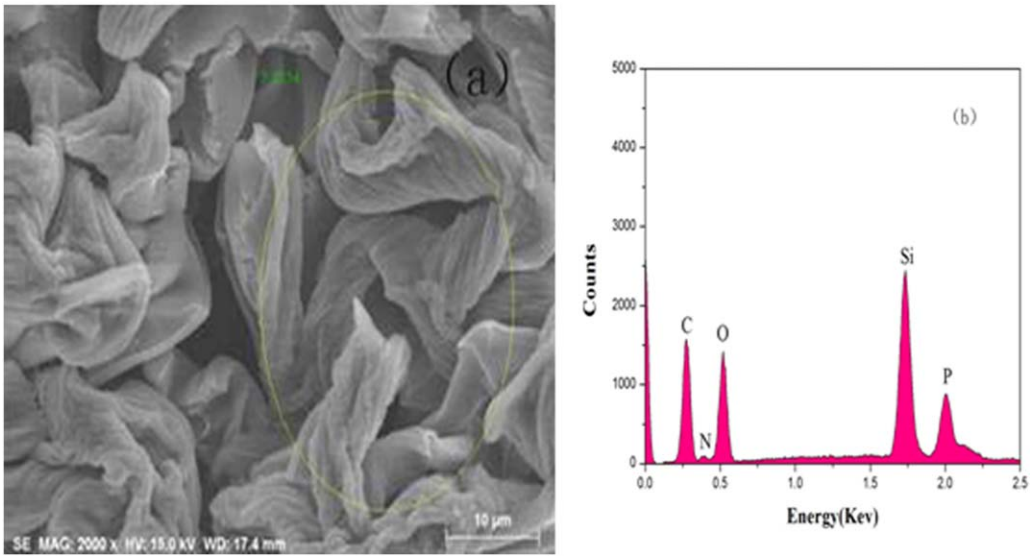

Figure 11. (a) SEM images and (b) EDS mapping pictures of the residue for the BDM/DBA/15% DP resin. [Color figure can be viewed in the online issue, which is available at wileyonlinelibrary.com.]

Figure 9 presents the SEM images of the residues acting as barriers. The residue morphology of BDM/DBA is given in Figure 9(a). As shown in the image, there were a few obvious surface cracks in the residue. These cracks were produced by the gas expansion rupture in the burning process; this suggests that the char was not tight enough to block gases and protect the matrix. Such a structure could not prevent the exchange of volatile gases and oxygen from the BDM/DBA resin decomposition; this resulted in only a V-1 classification for the BDM/DBA resin. Figure 9(b) shows the SEM image of the residual charred layer of the BDM/DBA/15% DP resin. The addition of DP enhanced the quality of the char layer. The surface of the charred layers became more integrated and compact. The residue of BDM/DBA/15% DP had a larger superficial area and contained extensive gases; this decreased the thermal conductivity and decreased the heat transfer. BDM/DBA/15% DP provided a V-0 classification because the compacted char effectively prevented the heat and mass transfer to the air between the condensed phase and the gas phase.

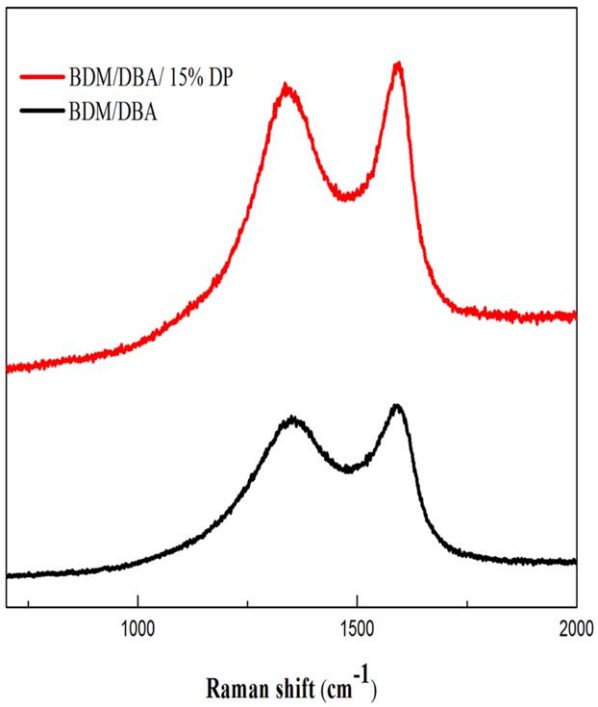

Figure 12. Raman curves of the char residues of BDM/DBA/*n*DP resins after they were maintained at 800°C for 15 min. [Color figure can be viewed in the online issue, which is available at wileyonlinelibrary.com.]

EDS Analysis of the Char

The chars produced from the BDM/DBA and BDM/DBA/15% DP resins were investigated by EDS analysis. The concentrations of C, O, N, Si, and P in the chars are listed in Table V. The atomic percentage of the C element in the char of BDM/DBA/15% DP was lower than that in the BDM/DBA resin, and the atomic percent of the O element in the char of BDM/DBA/15% DP was higher than that in the BDM/DBA resin. This was caused by the existence of abundant of Si—O_2 and P—O structures in the char. A number of Si and P elements were observed in the char of BDM/DBA/15% DP; this was helpful for enhancing the thermostability of the char.[35] This indicated that DP had obvious action in the condensed phase (Figures 10 and 11).

Table VI. *R* Values of the BDM/DBA and BDM/DBA/15% DP Resins in Raman Tests

Sample	*R*
BDM/DBA	3.03
BDM/DBA/15% DP	2.22

Effects of the Graphitization Degree of the Chars on the Flammability Properties

The microstructure of chars is a critical factor in the flammability properties of polymers. The degree of graphitization is a very important structural parameter; it reflects the transition extent of carbon material from a turbostratic to a graphitic structure and determines the properties of the material.

Raman spectroscopy has played an important role in the structural characterization of graphitic materials. There are two features in the Raman spectra of graphitic materials; these are the G band, appearing at 1582 cm^{-1} (graphite), and the D band, appearing at 1350 cm^{-1} (disordered char). Tuinstra and Koenig[36] pointed out that the ratio of the D and G band intensities ($R = I_D/I_G$) is inversely proportional to the in-plane crystallite sizes, which represent the graphitization degree of the chars.

Figure 12 shows the Raman diffusion spectra of the char residues of the BDM/DBA and BDM/DBA/15% DP resins after being maintained at 800°C for 10 min, and the *R* values of all resins are listed in Table VI. *R* decreased with a 15% loading of DP in BDM/DBA; this indicated that BDM/DBA/15% DP had a much higher degree of graphitization. The role of DP in the enhancement of the graphitization degree may have been its catalytic effect. The graphitization degree could be improved with such a catalyst. We concluded that a higher graphitization degree in the char structure showed a better thermooxidative stability for protecting the matrix. This is why the char yield increased with the addition of DP according to thermogravimetry testing.

Dielectric Properties of Cured BDM/DBA and BDM/DBA/DP Resins

Good dielectric properties are an important for resins, so it is necessary to test the dielectric properties of a modified resin for cutting-edge fields.

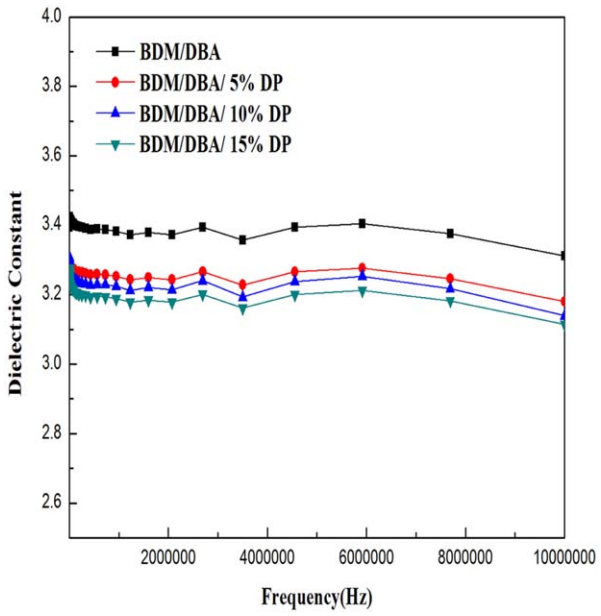

Figure 13. Dependence of the dielectric constant on the frequency of the cured BDM/DBA and BDM/DBA/*n*DP resins. [Color figure can be viewed in the online issue, which is available at wileyonlinelibrary.com.]

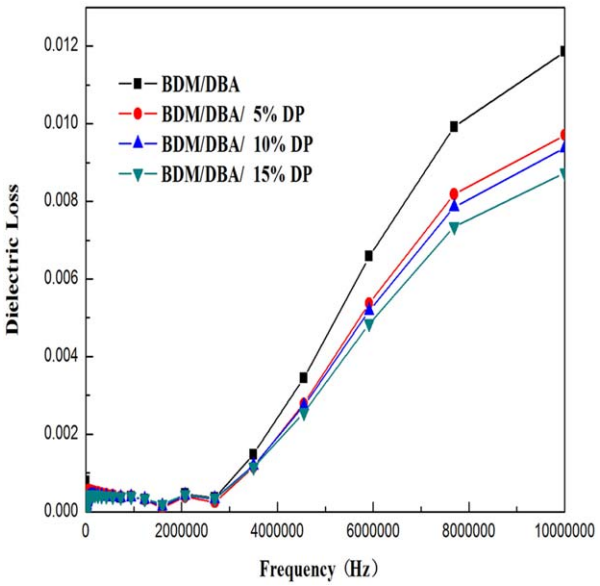

Figure 14. Dependence of the dielectric constant on the frequency of the cured BDM/DBA and BDM/DBA/*n*DP resins. [Color figure can be viewed in the online issue, which is available at wileyonlinelibrary.com.]

Figure 13 and 14 show the dependence of the dielectric constant and loss on the frequency for the cured BDM/DBA and BDM/DBA/DP resins, respectively. All of the BDM/DBA/DP resins exhibited very good stability of dielectric properties over a wide frequency range from 10^1 to 10^7 Hz, as the BDM/DBA resin did. Moreover, the former had a much lower dielectric constant and loss than the latter. On the other hand, the dielectric properties were greatly dependent on the content of DP, which increased as the content of DP increased. For example, the dielectric constant and loss of the BDM/DBA/15% DP resin at 1 MHz were 3.11 and 0.008, respectively, only about 93 and 73% of those of the BMI resin. This phenomenon was explained by the low polarity of Si—O—Si and the porous structure in the cage of DP.[37] DP as a flame retardant in the BDM/DBA resin also had a positive effect on the dielectric properties; this would be very attractive for actual applications

CONCLUSIONS

Flame-retardant BDM/DBA resins were obtained by the addition of a novel polyhedral oligomeric silsesquioxane containing DOPO into BDM/DBA. The fire-retardant properties of the BDM/DBA/DP resins were investigated and compared with those of the BDM/DBA resins. The addition of DP induced a fire-retardant effect in BDM/DBA and allowed it to obtain a V-0 classification in the UL-94 test. The mass results indicated that the BDM/DBA resin was consumed, and no solid residue remained at 800°C. The TGA results show that an increase in the DP loading had a positive effect on the thermal stability and char yield of the BDM/DBA resins. The Raman spectroscopy test suggested that the existence of DP enhanced the graphitization degree of BDM/DBA during combustion. The morphology and EDS analysis of the residue showed that the surface of the charred layers became more integrated and dense with the addition of DP. The compact char effectively prevented

the exchange of the heat and mass between the underlying polymer material and the flame zone. Moreover, the BDM/DBA/DP resin exhibited a lower dielectric constant and loss than BDM/DBA resin. This investigation demonstrated that high-performance resins with good flame retardancy and dielectric properties were developed by the addition of DP.

REFERENCES

1. Sun, B.; Liang, G. Z.; Gu, A. J.; Yuan, L. *Ind. Eng. Chem. Res.* **2013**, *52*, 5054.
2. Tsai, P. F.; Kuo, W. L.; Shau, M. D. *J. Chin. Chem. Soc.* **2013**, *60*, 229.
3. Xiong, L.; Lian, Z. Y.; Liang, H. B.; Huang, S. M.; Fan, H. Q. *Polym. Compos.* **2013**, *34*, 2154.
4. Shau, M.; Tsai, P. F.; Teng, W. Y.; Hsu, W. S. *Eur. Polym. J.* **2006**, *42*, 1899.
5. Chen, X. X.; Gu, A. J.; Liang, G. Z.; Yuan, L.; Zhuo, D. X.; Hu, J. T. *Polym. Degrad. Stab.* **2012**, *97*, 698.
6. Yang, C. W.; Liang, G. Z.; Gu, A. J.; Yuan, L. *Ind. Eng. Chem. Res.* **2013**, *52*, 15075.
7. Mariappan, T.; You, Z.; Hao, J. W.; Wilkie, C. A. *Eur. Polym. J.* **2013**, *49*, 3171.
8. Lorenzetti, A.; Besco, S.; Hrelja, D.; Roso, M.; Gallo, E.; Schartel, B.; Modesti, M. *Polym. Degrad. Stab.* **2013**, *98*, 2366.
9. Sullalti, S.; Colonna, M.; Berti, C.; Fiorini, M.; Karanam, S. *Polym. Degrad. Stab.* **2012**, *97*, 566.
10. Kumar, S. A.; Balakrishnan, T.; Alagar, A.; Denchev, Z. *Prog. Org. Coat.* **2006**, *55*, 207.
11. He, Q. L.; Lu, H. D.; Song, L.; Hu, Y.; Chen, L. J. *J. Fire Sci.* **2009**, *27*, 303.
12. Song, L.; He, Q. L.; Hu, Y.; Chen, H.; Liu, L. *Polym. Degrad. Stab.* **2008**, *93*, 627.
13. Neisius, N. M.; Lutz, M.; Rentsch, D.; Hemberger, P.; Gaan, S. *Ind. Eng. Chem. Res.* **2014**, *53*, 2889.
14. Artner, J.; Ciesielski, M.; Walter, O.; Doring, M.; Perez, R. M.; Sandler, J. K. W.; Altstadt, V.; Schartel, B. *Macromol. Mater. Eng.* **2008**, *293*, 503.
15. Nie, S. B.; Hu, Y.; Song, L.; He, Q. L.; Yang, D. D.; Chen, H. *Polym. Adv. Technol.* **2008**, *19*, 1077.
16. He, Q. L.; Song, L.; Hu, Y.; Zhou, S. *J. Mater. Sci.* **2009**, *44*, 1308.
17. Vannier, A.; Duquesne, S.; Bourbigot, S.; Castrovinci, A.; Camino, G.; Delobel, R. *Polym. Degrad. Stab.* **2008**, *93*, 818.
18. Baney, R. H.; Itoh, M.; Sakakibara, A.; Suzuki, T. *Chem. Rev.* **1995**, *95*, 1409.
19. Zhang, W.; Fang, B.; Walther, A.; Muüller, A. H. *Macromolecules* **2009**, *42*, 2563.
20. Liu, H.; Zhang, W.; Zheng, S. *Polymer* **2005**, *46*, 157.
21. Li, L. M.; Li, X. M.; Yang, R. J. *J. Appl. Polym. Sci.* **2012**, *124*, 3807.
22. Qian, Y.; Wei, P.; Zhao, X. M.; Jiang, P. K.; Yu, H. Z. *Fire Mater.* **2013**, *37*, 1.
23. Zhang, W.; Yang, R. *J. Appl. Polym. Sci.* **2011**, *122*, 3383.
24. Zhang, W. C.; Li, X. M.; Yang, R. *J. Polym. Degrad. Stab.* **2011**, *96*, 1821.
25. Zhang, W. C.; Li, X. M.; Yang, R. *J. Polym. Degrad. Stab.* **2012**, *97*, 1314.
26. Zhang, W.; Li, X.; Guo, X.; Yang, R. *Polym. Degrad. Stab.* **2010**, *95*, 2541.
27. Zhang, W.; Li, X.; Yang, R. *Polym. Degrad. Stab.* **2011**, *96*, 1821.
28. Li, Y. J.; Gu, X. Y.; Zhao, J.; Jiang, P.; Sun, J.; Wang, T. *J. Appl. Polym. Sci.* **2014**, *131*, 10.
29. Wang, X.; Hu, Y.; Song, L.; Xing, W. Y.; Lu, H. D. A.; Lv, P.; Jie, G. X. *Polymer* **2010**, *51*, 2435.
30. Zeng, J. *High Perform. Polym.* **2005**, *17*, 403.
31. Lu, S. Y.; Hamerton, I. *Prog. Polym. Sci.* **2002**, *27*, 1661.
32. Wu, K.; Song, L.; Hu, Y.; Lu, H.; Kandola, B. K.; Kandare, E. *Prog. Org. Coat.* **2009**, *65*, 490.
33. Wang, X.; Hu, Y.; Song, L.; Xing, W.; Lu, H. *J. Polym. Sci. Part B: Polym. Phys.* **2010**, *48*, 693.
34. Zhuo, D. X.; Gu, A. J.; Liang, G. Z.; Hu, J. T.; Yuan, L.; Chen, X. X. *J. Mater. Chem.* **2011**, *21*, 6584.
35. Chow, W.; Neoh, S. *J. Appl. Polym. Sci.* **2009**, *114*, 3967.
36. Tuinstra, F.; Koenig, J. L. *J. Chem. Phys.* **2003**, *53*, 1126.
37. Hu, J. T.; Gu, A. J.; Jiang, Z. J.; Liang, G. Z.; Zhuo, D. X.; Yuan, L.; Zhang, B. J.; Chen, X. X. *Polym. Adv. Technol.* **2012**, *23*, 1219.